Ezh1 regulates expression of *Cpg15/Neuritin* in mouse cortical neurons

Shun Utsunomiya[1,2,3,4,§]**, Yusuke Kishi**[1,§]**, Masafumi Tsuboi**[2]**, Daichi Kawaguchi**[1]**, Yukiko Gotoh**[1,5]**, Manabu Abe**[6]**, Kenji Sakimura**[6]**, Kazuma Maeda**[3,4]**, Hiroshi Takemoto**[3,4,*]

[1] Graduate School of Pharmaceutical Sciences, The University of Tokyo, Tokyo, Japan;
[2] Graduate School of Engineering, The University of Tokyo, Tokyo, Japan;
[3] Neuroscience 2, Laboratory for Drug Discovery and Disease Research, Shionogi & Co. Ltd., Toyonaka, Osaka, Japan;
[4] Business-Academia Collaborative Laboratory (Shionogi), Graduate School of Pharmaceutical Sciences, The University of Tokyo, Tokyo, Japan;
[5] International Research Center for Neurointelligence (WPI-IRCN), The University of Tokyo, Tokyo, Japan;
[6] Department of Animal Model Development, Brain Research Institute, Niigata University, Niigata, Japan.

SUMMARY   Immature neurons undergo morphological and physiological maturation in order to establish neuronal networks. During neuronal maturation, a large number of genes change their transcriptional levels, and these changes may be mediated by chromatin modifiers. In this study, we found that the level of Ezh1, a component of Polycomb repressive complex 2 (PRC2), increases during neuronal maturation in mouse neocortical culture. In addition, conditional knockout of Ezh1 in post-mitotic excitatory neurons leads to downregulation of a set of genes related to neuronal maturation. Moreover, the locus encoding Cpg15/Neuritin (Nrn1), which is regulated by neuronal activity and implicated in stabilization and maturation of excitatory synapses, is a direct target of Ezh1 in cortical neurons. Together, these results suggest that elevated expression of Ezh1 contributes to maturation of cortical neurons.

Keywords   epigenetics, Polycomb group proteins, neuronal maturation, depression, Alzheimer's disease, Nrn1

1. Introduction

The mammalian neocortex processes various kinds of information and governs higher-order functions such as behavior and cognition. Neurons are the most fundamental elements of the brain, and in order for the brain to perform its higher-order brain functions, they must form intricate networks. To this end, neurons must undergo dramatic maturation processes. During neocortical development, neurons are generated from neural precursor cells (NPCs) and migrate toward the pial surface (*1*). After reaching the pia, they stop migration and undergo dramatic morphological and functional maturation, including outgrowth of axons and dendrites, synapse formation, and establishment of membrane potential (*2-4*). The processes of neuronal fate decision and maturation into elaborate neurons involves the products of many genes. Indeed, global patterns of gene expression change during neuronal maturation (*5*): microarray analysis revealed that 49% of 14,213 mRNAs in mouse neocortex change their expression levels during this process. It remains unclear, however, how genome-wide transcription pattern is coordinately regulated during this maturation process.

Chromatin-level mechanisms such as DNA methylation and histone modifications play important roles in transcriptional regulation (*6-8*). Chemical modifications at histone tails change the chromatin state, leading to transcriptional activation or repression. For example, tri-methylation of histone H3 at lysine-4 (H3K4me3) is associated with transcriptional activation, whereas H3K9me3 and H3K27me3 are associated with transcriptional repression. Polycomb group (PcG) proteins are chromatin modifiers that regulate gene expression patterns, primarily through transcriptional repression. PcG assemble to form two protein complexes, polycomb repressive complex 1 (PRC1) and PRC2. These complexes catalyze ubiquitylation of histone 2A at lysine-119 (H2AK119ub) and trimethylation of histone 3 at lysine-27 (H3K27me3), respectively (*9,10*). PRC2-mediated H3K27me3 plays critical roles in the stage-specific repression of developmental regulator genes, and frequently exhibits bivalency along with an active histone modification, H3K4me3, during cellular differentiation (*11,12*).

The core components of PRC2 are Eed, Suz12, and the H3K27me3 transferase enhancer of zeste homolog

(Ezh) 1 or 2. Although the catalytic SET domains of Ezh1 and Ezh2 are highly homologous to each other, the H3K27me3 transferase activity of Ezh1 is much weaker than that of Ezh2 in NIH3T3 cells (*13*). To function, Ezh proteins must form complexes with other PRC2 components (*13-15*). Ezh1 and Ezh2 compete for other PRC2 components, and are therefore mutually exclusive in complex formation (*13-15*). Moreover, the expression patterns of Ezh1 and Ezh2 tend to be mutually exclusive. Expression of Ezh2 is frequently associated with a proliferative state (*16,17*), whereas Ezh1 is primarily expressed in post-mitotic or quiescent cells including hippocampal neurons, medium spiny neurons (MSNs) in the striatum, myotubes, aging kidney, and hematopoietic stem cells (*13,15,18-22*). Although Ezh proteins are primarily associated with gene repression through PRC2, several lines of evidence suggest that they also play non-canonical roles in gene activation in a context-dependent manner (*15,18,20,21*). However, in cortical neurons, whether expression levels of PRC2 components including Ezh proteins are changed, and whether Ezh proteins repress or activate their target genes are not investigated.

In NPCs, PRC2 plays various roles in maintaining the undifferentiated state of NPCs and temporal regulation of their fate restriction (*23-25*). The functions of PRC2 during neuronal maturation have also been explored. For example, in a rat hippocampal neuronal culture, knockdown of Ezh2 derepresses transcription of PSD95, a postsynaptic marker in excitatory neurons, and decreases secondary and tertiary branching of dendrites, whereas knockdown of Ezh1 decreases transcription of PSD95 (*18*). In addition, knockdown of Ezh2 increases neuronal firing frequency and febrile seizure susceptibility *in vivo* (*26*). Conditional knockout of *Ezh2* in neural progenitors results in derepression of HoxPG5 and Netrin-1 and aberrant pontine neuronal migration (*27*). In mature MSNs, PRC2 contributes to suppression of a transcriptional program that is detrimental to adult neuron function and survival (*22*). Knockdown of Ezh1 in the adult mouse prefrontal cortex attenuates sociability and promotes motivational behaviors (*28*). Therefore, it is of interest to determine which targets can be regulated by Ezh1 in postmitotic neurons.

In this study, we investigated the role of Ezh1 in the maturation of mouse neocortical neurons in an *in vitro* culture system. To this end, we generated a mouse line in which *Ezh1* could be conditionally deleted. We found that expression of Ezh1 increased during neuron maturation in primary neocortical culture. Moreover, neuron-specific deletion of *Ezh1* resulted in downregulation of a set of genes related to neuronal maturation. Among these genes, Ezh1 directly associated with the locus encoding Cpg15/Neuritin (Nrn1), which is regulated by neuronal activity and mediates the neuronal maturation process. Our results suggest that Ezh1 contributes to neuronal maturation by regulating expression of Nrn1.

2. Materials and Methods

2.1. Animals

All animals were maintained and studied according to protocols approved by the Animal Care and Use Committee of The University of Tokyo (approval numbers: P25-8 and P30-4). *Ezh1^flox/flox^* mice, described below, were crossed with *NEX-Cre* transgenic mice (*29*). JCL: ICR (CLEA Japan, Tokyo, Japan) or Slc: ICR (SLC Japan, Shizuoka, Japan) mice were used as wild-type animals. All mice were maintained in a temperature- and relative humidity-controlled environment (23 ± 3°C and 50 ± 15%, respectively) with a normal 12-h-light, 12-h-dark cycle. Two to six animals were housed per sterile cage (Innocage, Innovive, Sandiego, CA, USA) with chips (PALSOFT, Oriental Yeast, Tokyo, Japan), and with irradiated food (CE-2, CLEA Japan) and filtered water were available ad libitum.

2.2. Production of *Ezh1^flox/flox^* mice

All experiments were performed according to protocols approved by the Animal Care and Use Committee of The University of Tokyo and Niigata University. The *Ezh1^flox/flox^* mouse line was produced by homologous recombination using the ES cell line RENKA, which was developed from the C57BL/6N strain (*30*). The targeting vector was constructed in accordance with the mouse genomic DNA databases contained from exon 2 to exon 7 of *Ezh1* gene with the 6.76 kb upstream and 6.26 kb downstream (Figure 2a; exons are indicated by boxes with the exon number above). The neomycin phosphotransferase gene (*Neo*) and the gene encoding fragment A of diphtheria toxin (*DT-A*) were included for positive and negative selection, respectively. A DNA fragment containing a 34-bp loxP sequence and *Pgk1* promoter-driven *Neo* flanked by a pair of flippase recombinase target (FRT) sequences was inserted 1523 bp upstream of exon 5. The other loxP site was introduced 1,063 bp downstream of exon 2. Thus, Cre-loxP deletion would delete exons 3 and 4, resulting in a nonsense mutation in the *Ezh1* gene. Introduction of the targeting vector into mouse ES cells, screening for homologous recombinants with southern blot analysis, production of chimeric mice, were carried out as described previously (*30*). A diagnostic external probe for southern blot analysis is shown in a thick line. The resultant chimeric mice were mated with C57BL/6N mice, and offspring [*Ezh1^+/lox(neo)^*] were further crossed with *Actb-Flp* mice to remove the neo cassette. The *flp* gene was bred out in the next generation. After confirming deletion of the neo cassette, heterozygous (*Ezh1^flox/+^*) mice were mated to generate homozygous (*Ezh1^flox/flox^*) mice. PCR genotyping was performed using primers 5'- AGATTGCAGGCATTCTCTGT -3' (forward) and 5'- TGTCGAAGCCGCATATACTC -3' (reverse),

which yielded PCR products of 530 bp for the floxed allele and 430 bp for the wild-type allele.

2.3. Primary neuron culture

The cortex was isolated from ICR mice at E14.5 or *NEX-Cre*$^{-/- \text{ or } +/-}$; *Ezh1*$^{flox/flox}$ mice at E15.5, with the appearance of the vaginal plug considered to be E0.5. Dissected cortices were subjected to enzymatic digestion with a papain-based solution (FUJIFILM Wako chemicals, Tokyo, Japan), and the dissociated cells were plated directly and cultured on dishes coated with poly-D-lysine (Sigma-Aldrich, St. Louis, MO, USA) and were maintained in differentiation-inducing medium, which contains Neurobasal (Thermo Fisher Scientific, Waltham, MA, USA) and Neuron Culture Medium (FUJIFILM Wako chemicals), supplemented with B27 and GlutaMAX (Thermo Fisher Scientific), for several days. At 5 or 6 days in vitro (DIV), half of the medium was replaced, and cytosine arabinoside (Sigma-Aldrich) were added to the culture medium at a concentration of 5 μM to prevent expansion of glial cells.

Genotypes of *NEX-Cre*$^{-/- \text{ or } +/-}$; *Ezh1*$^{flox/flox}$ mice were evaluated after plating. Tissue from each embryo was collected and lysed with 50 mM NaOH, and then incubated at 98°C for 10 min. After mixing with 1 M Tris-HCl (pH 8.0), each lysate was subjected to PCR using KOD-FX polymerase (Toyobo, Osaka, Japan). PCR primers for *Nex-Cre* are described in (*29*).

2.4. Reverse transcription-quantitative PCR analysis

Total RNA was isolated from cells using Trizol (Thermo Fisher Scientific) or RNA IsoPlus (Toyobo), and up to 0.5 μg of the RNA was subjected to RT using ReverTra Ace qPCR RT Master Mix with gDNA Remover (Toyobo). The resultant cDNA was subjected to real-time PCR analysis in a LightCycler 480 instrument (Roche, Basel, Switzerland) with Thunderbird SYBR qPCR mix (Toyobo). The level of each target mRNA was normalized against the corresponding level of *Actb* mRNA. Primer sequences are provided in Table S1 (*http://www.ddtjournal.com/action/getSupplementalData. php?ID=69*).

2.5. Immunoblot analysis

Cells were lysed with RIPA buffer containing 50 mM Tris- HCl (pH 7.5), 150 mM NaCl, 1% NP-40, 0.5% sodium-deoxycholate, 0.1% SDS, and protease-inhibitor (1 mg/mL). The lysates were subjected to immunoblot analysis with antibodies against Cre (1:500 dilution; 69050, Novagen, Darmstadt, Germany), Ezh1 (1:500; HPA005478, Sigma-Aldrich or 1:500; 20852-1-AP, Protein-tech, Tokyo, Japan), H3 (1:2,000; ab1791, Abcam, Cambridge, UK), H3K27me3 (1:1,000; 07-449, Millipore, Darmstadt, Germany or 1:1,000; 9733, CST,

Danvers, MA, USA), and ßIII-tubulin (1:1,000; MMS-435P, Covance, Princeton, NJ). Immune complexes were detected with horseradish peroxidase conjugated secondary antibodies (GE Healthcare, Chicago, IL, USA) and Luminata Forte Western HRP substrate or Immobilon ECL Ultra Western HRP Substrate (Millipore) on an Image Quant LAS4000 instrument (GE Healthcare). Band intensities were measured using the ImageJ Software.

2.6. Chromatin immunoprecipitation-quantitative PCR analysis

Chromatin immunoprecipitation (ChIP) for Ezh1 and H3K27me3 was carried out as described in (*31*). Cells were fixed with 1% formaldehyde and stored at –80°C until analysis. The cells were thawed, suspended in RIPA buffer for sonication (10 mM Tris-HCl at pH 8.0, 1 mM EDTA, 140 mM NaCl, 1% Triton X-100, 0.1% SDS, and 0.1% sodium deoxycholate) and subjected to ultrasonic treatment on a Picoruptor (15 cycles of 30 s ON and 30 s OFF) (Diagenode, Seraing, Belgium). Cell lysates were then diluted with RIPA buffer for immunoprecipitation (50 mM Tris-HCl at pH 8.0, 150 mM NaCl, 2 mM EDTA, 1% Nonidet P-40, 0.1% SDS, and 0.5% sodium deoxycholate) and incubated for 1 h at 4°C with Protein A/G Magnetic Beads (Pierce, Waltham, MA, USA) to clear non-specific reactivity. They were then incubated overnight at 4°C with Protein A/G Magnetic Beads that had previously been incubated for overnight at 4°C with antibodies. The beads were isolated and washed first three times with wash buffer (2 mM EDTA, 150 mM NaCl, 0.1% SDS, 1% Triton X-100, and 20 mM Tris-HCl at pH 8.0) and then once with wash buffer containing 500 mM NaCl. Immune complexes were eluted from the beads for 15 min at 65°C with a solution containing 10 mM Tris-HCl at pH 8.0, 5 mM EDTA, 300 mM NaCl, and 0.5% SDS, and they were then subjected to digestion with proteinase K (Nacalai Tesque, Kyoto, Japan) for > 6 h at 37°C, removal of cross links by incubation for > 6 h at 65°C, and extraction of the remaining DNA with phenol-chloroform-isoamyl alcohol and ethanol. The DNA was washed with 70% ethanol, suspended in water, and subjected to real-time PCR analysis in a LightCycler 480 (Roche) with Thunderbird SYBR qPCR Mix (Toyobo). Primer sequences are provided in Table S2 (*http://www.ddtjournal.com/action/ getSupplementalData.php?ID=69*).

2.7. RNA-seq analysis

Libraries for RNA-seq analysis were constructed from total RNA isolated as described above for RT-qPCR analysis. The SMART-seq stranded kit (Takara, Shiga, Japan) was used for template preparation, followed by deep sequencing on the Illumina HiSeqX platform to obtain 151-base paired-end reads. Approximately 10-

50 million sequences were obtained from each sample. Sequences were mapped to the reference mouse genome (mm10) with Hisat2 (*32*). Only uniquely mapped tags with no base mismatches were used for the analysis. Reads in each gene locus were counted using the featureCounts software (*33*) and gene expression levels were quantitated as reads per kilobase of mRNA model per million total reads (RPKM). Differentially expressed genes (DEGs) were identified using *edgeR* from the *R* package (*34,35*) as genes whose *q* values were < 0.25. GO analysis was carried out using DAVID Bioinformatic Resources (*36,37*), and GO terms whose Benjamini score was < 0.25 were considered as significant.

2.8. Statistical analysis

Data are presented as means ± SEM and were compared with the two-tailed Student's unpaired *t* test or by analysis of variance (ANOVA) followed by Dunnett's multiple-comparison test.

2.9. Data availability statement

The sequence data have been deposited in the DNA Data Bank of Japan (DDBJ) Sequence Read Archive under the following ID: DRA011526.

3. Results

3.1. Expression of PRC2 components changes during maturation of cortical neurons *in vitro*

Expression levels of PRC2 components have been investigated in MSNs in the mouse striatum, as well as in rat hippocampal neurons (*18,22*), but not in the cortical neurons. Hence, we investigated whether expression of PRC2 components changes during maturation of mouse neocortical neurons. To this end, we first examined mRNA levels of PRC2 core components by reverse transcription-quantitative PCR (RT-qPCR) (Figure 1a). We prepared primary neuronal cultures isolated from E14.5 neocortex and cultured them for several days *in vitro* (DIV) in a differentiation-inducing medium. Expression of *Tubb3*, a neuronal marker, was higher at 7 DIV *vs.* 1 DIV, suggesting that neuronal maturation had progressed (Figure 1a). By contrast, the levels of *Eed* and *Suz12* mRNA did not significantly change between at 1 and 7 DIV (Figure 1a). The level of *Ezh1* mRNA increased at 7 DIV *vs.* 1 DIV, whereas the level of *Ezh2* decreased (Figure 1a). Next, we examined protein level of *Ezh1* (Figures 1b and 1c). Immunoblot analysis revealed that expression of βIII-tubulin increased at 7 DIV *vs.* 0 DIV (Figures 1b and 1c). Also, the level of Ezh1 proteins increased at 7 DIV *vs.* 0 DIV along with the level of *Ezh1* mRNA (Figures 1b and 1c). On the other hand, the level of H3K27me3 did not significantly change at 7 DIV *vs.* 0 DIV (Figures 1b and 1c). Together,

these results suggest that expression of Ezh1 increases during the maturation of neocortical neuron.

3.2. Establishment of an excitatory neuron specific knockout of Ezh1

Given that the expression level of Ezh1 increases during neuronal maturation, we investigated the possible roles of Ezh1 during this process. For this purpose, we generated a mouse strain (*Ezh1^{flox/flox}*) in which loxP sequences were inserted downstream of exon 2 and upstream of exon 5 (Figure 2a and 2b). We then induced conditional knockout of the *Ezh1* gene specifically in post-mitotic excitatory neurons by crossing *Ezh1^{flox/flox}* mice with *NEX-Cre* transgenic mice, which express Cre recombinase in differentiating excitatory neurons under the control of the *Math2* (*Neurod6*) promoter (*29,38*). Before conducting experiments, we first confirmed the deletion of *Ezh1* by this conditional KO (cKO). Immunoblotting of extracts from neocortical culture isolated from E15.5 cortex and cultured for 10 DIV revealed that the level of Ezh1 protein significantly decreased following Ezh1 cKO (Figure 2c), indicating that *Ezh1* was successfully deleted. Interestingly, the global level of H3K27me3 was not significantly reduced by Ezh1 cKO (Figures 2c and 2d), implying the existence of compensatory mechanisms or slow turnover of H3K27me3 in these cells.

3.3. Transcriptional changes caused by Ezh1 cKO in cortical neurons *in vitro*

Next, using the newly-established Ezh1 cKO mice, we examined the effects of *Ezh1* deletion on gene expression patterns. Specifically, we conducted RNA sequencing (RNA-seq) analysis and compared the gene expression patterns of control and Ezh1 cKO cortical neurons. For these experiments, we prepared E15.5 neocortices from either control or Ezh1 cKO mice and cultured them for 10 DIV under differentiation-inducing conditions. We analyzed differentially expressed genes (DEGs) determined using *edgeR* of the *R* package (*34,35*). We identified upregulated DEGs (3059) and downregulated DEGs (1626) in neocortical neuronal cultures from Ezh1 cKO mice relative to those from control mice (Figures 3a and 3b). In contrast to previous reports on rat hippocampal neurons (*18*), expression of *Dlg4/PSD95* did not significantly change following Ezh1 cKO in our cortical cultures (Table 1). To explore the possibility that Ezh1 contributes to neuronal maturation, we performed Gene Ontology (GO) analysis for both upregulated and downregulated gene sets using the DAVID Bioinformatic Resources (*36,37*) (Figures 3c and 3d). Genes upregulated by Ezh1 cKO were enriched for many non-neuronal GO terms, including defense response, system process, cytokine production, cell activation, and response to external stimulus (Figure 3c). *Ezh1* and *Ezh2* double knockout in MSNs leads to derepression of non-
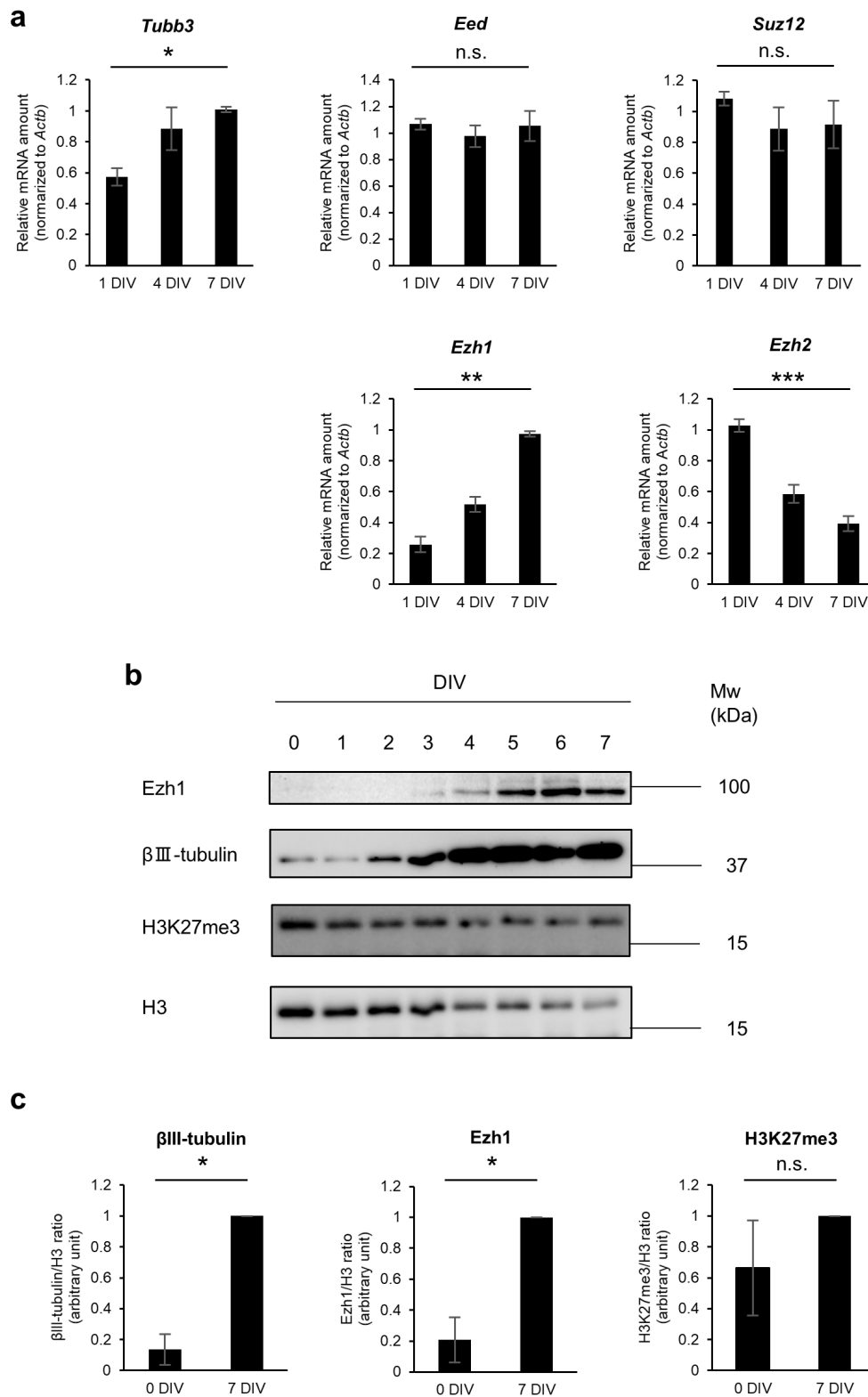
Figure 1. Changes in expression levels of PRC2 components during neuronal maturation *in vitro*. (a) RT-qPCR analysis of *Tubb3* (neuronal marker) and PRC2 components, *Ezh1*, *Ezh2*, *Eed*, and *Suz12* in cortical neurons isolated from E14.5 mouse cortex and cultured for 1 to 7 DIV under differentiation-inducing conditions. RT-qPCR data for each mRNA were normalized against the corresponding levels of *Actb* mRNA; means ± SEM from three independent experiments are shown. *$p < 0.05$, **$p < 0.01$, ***$p < 0.001$ (two-tailed unpaired Student's *t*-test). **(b), (c)** Immunoblot analysis with antibodies against the indicated proteins in cortical neurons isolated from E14.5 mouse cortex and cultured for 0 to 7 DIV under differentiation-inducing conditions. The representative images of three independent experiments are shown in **(b)**. Quantifications of each amount of βIII-tubulin, Ezh1, and H3K27me3 normalized against the corresponding levels of H3 at 0 and 7 DIV are shown in **(c)**; means ± SEM from three independent experiments are shown. *$p < 0.05$ (two-tailed unpaired Student's *t*-test).
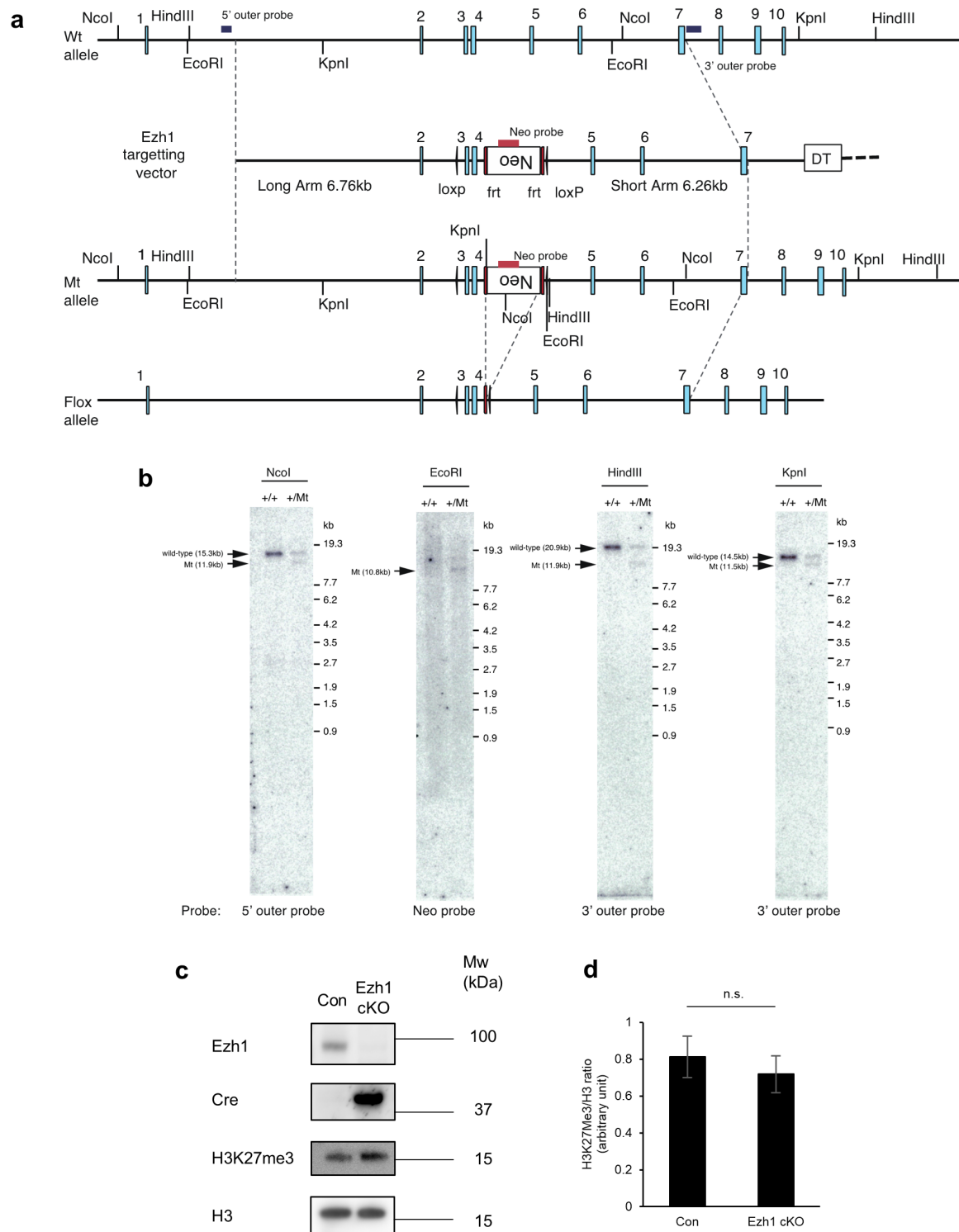
Figure 2. Establishment of excitatory neuron specific knockout of *Ezh1*. (a) Conditional disruption of the mouse *Ezh1* gene locus. Schematic representations show the wild-type allele, the targeting vector, and the resultant mutant and floxed alleles. **(b)** Southern blot analysis of ES cells of the indicated genotypes, using the indicated probes and restriction enzymes. **(c)** Immunoblot analysis with antibodies against the indicated proteins in cortical neurons isolated from *NEX-Cre*[-/- or +/-]; *Ezh1*[flox/flox] E15.5 mouse cortex and cultured for 10 DIV under differentiation-inducing conditions. **(d)** Quantification of H3K27me3/H3 ratio. Data are means ± SEM from three independent samples (two-tailed unpaired Student's *t*-test).
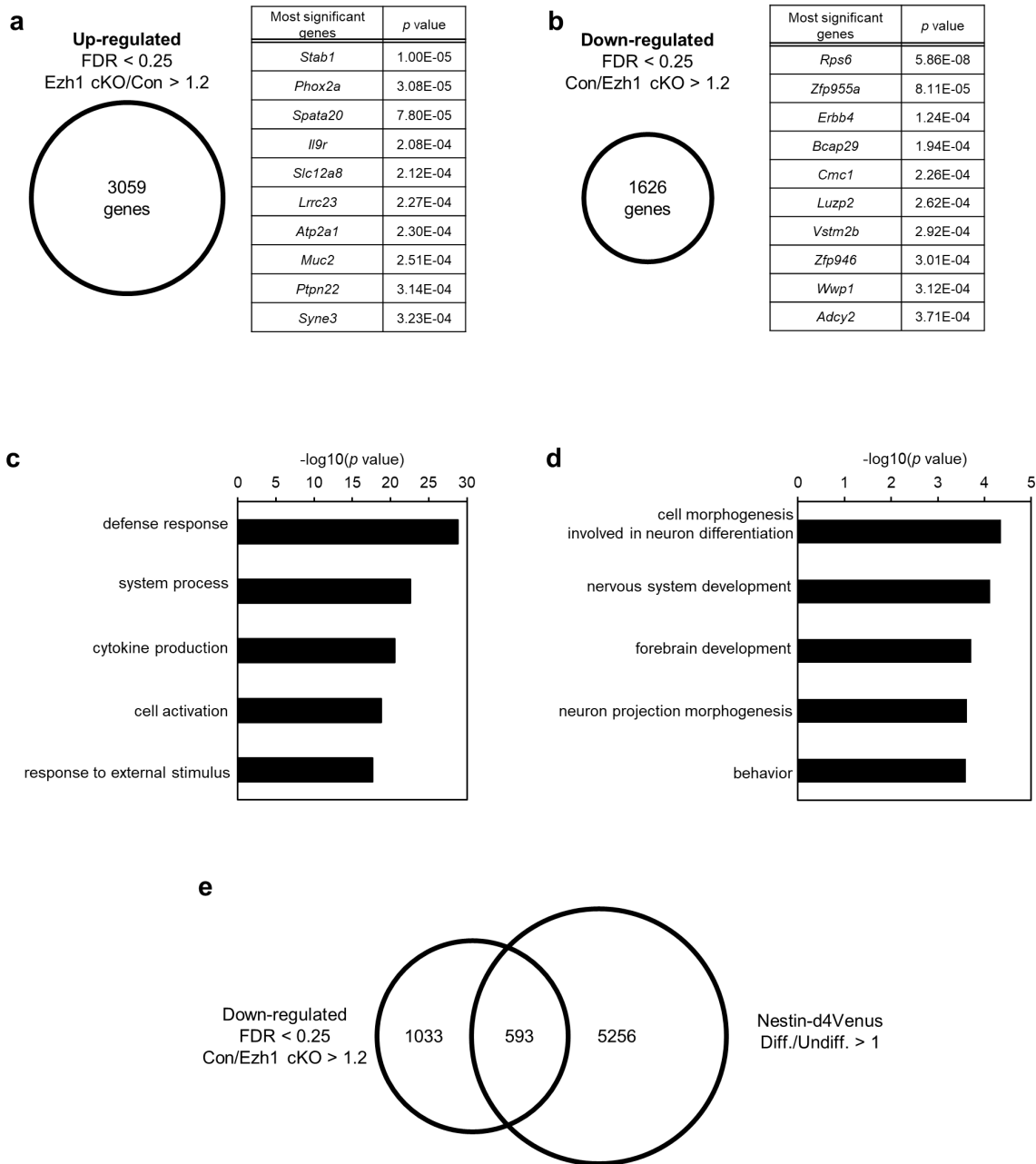
a

Up-regulated
FDR < 0.25
Ezh1 cKO/Con > 1.2

3059 genes

Most significant genes	*p* value
Stab1	1.00E-05
Phox2a	3.08E-05
Spata20	7.80E-05
Il9r	2.08E-04
Slc12a8	2.12E-04
Lrrc23	2.27E-04
Atp2a1	2.30E-04
Muc2	2.51E-04
Ptpn22	3.14E-04
Syne3	3.23E-04

b

Down-regulated
FDR < 0.25
Con/Ezh1 cKO > 1.2

1626 genes

Most significant genes	*p* value
Rps6	5.86E-08
Zfp955a	8.11E-05
Erbb4	1.24E-04
Bcap29	1.94E-04
Cmc1	2.26E-04
Luzp2	2.62E-04
Vstm2b	2.92E-04
Zfp946	3.01E-04
Wwp1	3.12E-04
Adcy2	3.71E-04

c

-log10(*p* value)

GO term	
defense response	
system process	
cytokine production	
cell activation	
response to external stimulus	

d

-log10(*p* value)

GO term	
cell morphogenesis involved in neuron differentiation	
nervous system development	
forebrain development	
neuron projection morphogenesis	
behavior	

e

Down-regulated
FDR < 0.25
Con/Ezh1 cKO > 1.2

1033   593   5256

Nestin-d4Venus
Diff./Undiff. > 1

Figure 3. Genome-wide gene expression analysis of Ezh1 cKO cortical neurons. (a and **b)** Cortical neurons were isolated from the *NEX-Cre^{-/-}*; *Ezh1[flox/flox]* (Control) or *NEX-Cre^{+/-}*; *Ezh1[flox/flox]* (Ezh1 cKO) E15.5 mouse cortex and cultured for 10 DIV under differentiation-inducing conditions. Genes whose expression was upregulated **(a)** or downregulated **(b)** by Ezh1 cKO were defined as those whose Ezh1 cKO/control or control/ Ezh1 cKO fold change was > 1.2 on average, with a false discovery rate (FDR) of 0.25. The genes with the 10 lowest *p* values (determined with *edgeR*) in each category are also listed (right panels). **(c** and **d)** Enriched GO terms and their *p* values, determined by functional annotation of all upregulated DEGs **(c)** and all downregulated DEGs **(d)** using the DAVID software. **(e)** Venn diagram representing the overlap between DEGs downregulated by Ezh1 cKO and genes expressed more strongly in d4Venus^{-} cells (differentiated neurons) than in d4Venus^{high} cells (undifferentiated NPCs).

MSN and non-neuronal lineage-specific transcription factors (*22*). Similarly, our gene expression data suggest that non-neuronal genes were upregulated by Ezh1 cKO.

Because Ezh1 can positively regulate the transcription of some target genes in addition to playing its conventional role as a transcription repressor (*15,18,20,21*), we next focused on genes that were downregulated gene by Ezh1 cKO. Downregulated DEGs were enriched for

neuron-related terms like cell morphogenesis involved in neuron differentiation, nervous system development, forebrain development, neuron projection morphogenesis, and behavior (Figure 3d), indicating that Ezh1 cKO decreases expression of genes related to neuronal maturation. To find genes related to neuronal maturation that were regulated by Ezh1, we combined our RNA-seq data with a dataset obtained by comparing FACS-

Table 1. The list of representative genes downregulated by Ezh1 cKO

Gene Symbol	Con [rpkm]	Ezh1 cKO [rpkm]	Ezh1 cKO/Con	*p* value	Excitatory or Inhibitory
Erbb4	7.80	4.49	0.576	1.24E-04	Inhibitory
Kcnt2	11.46	7.04	0.614	4.55E-04	Excitatory
Epha3	11.22	7.46	0.665	5.16E-04	Both
Nptx2	8.96	5.48	0.612	6.21E-04	Excitatory
Cntnap2	9.63	6.57	0.682	6.23E-04	Both
Zfp804a	18.28	10.17	0.557	6.58E-04	Inhibitory
Gabra1	25.59	17.08	0.667	9.90E-04	Both
Ube3a	16.38	10.58	0.646	1.36E-03	Both
Lin7a	8.71	4.58	0.525	1.41E-03	Both
Grin2b	31.69	19.15	0.604	1.58E-03	Both
Neurod6(NEX)	57.29	41.51	0.725	1.80E-03	Excitatory (Control)
Grik3	9.88	7.72	0.782	3.58E-03	Both
Nrn1	13.65	10.54	0.772	4.31E-03	Excitatory
Nptx1	7.43	5.68	0.765	5.43E-03	Excitatory
Maf	5.27	4.14	0.786	7.36E-03	Inhibitory
Gad2	21.54	15.72	0.730	1.90E-02	Inhibitory
Dlg4(PSD95)	27.55	30.96	1.124	5.54E-01	Both (*18*)

List of representative genes that were downregulated by Ezh1 cKO and expressed more strongly in d4Venus⁻ cells (differentiated neurons) than in d4Venus^high cells (undifferentiated NPCs) and are related to neuronal maturation. The table shows average RPKM (reads per kilobase of mRNA per million total reads) of control or Ezh1 cKO three samples and *p* values (determined with *edgeR*). Judgement for genes expressed mainly in excitatory neurons, expressed mainly in inhibitory neurons, or expressed in both excitatory and inhibitory neurons is based on (*48*).

separated undifferentiated cells and differentiated cells from *Nestin-d4Venus* transgenic mice at E14.5 (*39*). A total of 593 genes that were downregulated by Ezh1 cKO were also more highly expressed in differentiated cells than in undifferentiated cells (Figure 3e). The set of DEGs that were downregulated by Ezh1 cKO included genes expressed mainly in excitatory neurons such as *Kcnt2*, *Nptx1*, *Nptx2*, and *Nrn1*, genes expressed mainly in inhibitory neurons such as *Erbb4*, *Gad2*, *Maf*, and *Zfp804a*, and genes expressed in both excitatory and inhibitory neurons such as *Cntnap2*, *Epha3*, *Gabra1*, *Grik3*, *Grin2b*, *Lin7a*, and *Ube3a*, all of which have been implicated in regulation of neuronal maturation (Table 1). Because we constructed the cKO mice with *NEX-Cre* mice, in which Cre is exclusively expressed in excitatory neurons (*29*), we expected *Ezh1* to be knocked out specifically in excitatory neurons and guessed that Ezh1 directly regulates gene expression in excitatory neurons. Therefore, downregulation of a set of genes mainly expressed in inhibitory neurons might not be a direct effect by Ezh1 cKO, but might be a secondary effect by changing transcriptional status of excitatory neurons by Ezh1 cKO. These results suggest that *Ezh1* deletion decreases the expression levels of a set of genes related to neuronal maturation.

3.4. Ezh1 binds directly to the promoter of *Nrn1*

Given the dysregulation of neuronal maturation-related gene expression induced by *Ezh1* deletion, we next investigated whether these genes, especially excitatory neuron-related genes, were direct targets of PcG proteins. To this end, we performed ChIP-qPCR assays for H3K27me3, a histone modification catalyzed by PRC2, as well as for Ezh1, on neocortical cultures

prepared from wild-type mice at E14.5 and cultured for 10 DIV under differentiation-inducing conditions. Among the genes related to neuronal maturation mentioned above, *Cpg15/Nrn1* is a direct target of several PRC1 components in human fibroblasts (*40*), but it remains unknown whether this gene is a target of PcG components in neurons. *Cpg15/Nrn1* is an activity-regulated gene whose expression in the mammalian cortex is experience-dependent (*41,42*), and it is necessary for experience-dependent spine and synapse stabilization (*43*). Knockout mice exhibit developmental delays in synapse formation and poor learning (*44*) and aberrant plasticity in visual cortical networks (*45*). We detected significant deposition of H3K27me3 at the promoter of *Nrn1* at levels similar to those apparent at the promoter of *Hoxd3* (a positive control) (Figure 4a). Also, we detected Ezh1 at the promoter of *Nrn1* (Figure 4b). These results suggest that Ezh1 directly upregulates the expression of *Nrn1* in neocortical neurons.

4. Discussion

In this study, we found that expression of Ezh1 increases during neuronal maturation in the mouse neocortical culture, as in hippocampal neurons and medium spiny neurons (*18,22*). In addition, we found that excitatory neuron-specific knockout of Ezh1 leads to downregulation of a set of genes related to neuronal maturation. Finally, we identified the *Nrn1* promoter as a novel target of Ezh1 in neurons.

Previous studies in rat hippocampal neurons and mouse MSNs show that the level of Ezh2 decreases during neuronal maturation, whereas that of Ezh1 does not (*18,22*). Our results are consistent with these reports. In addition, we showed that Ezh1 regulates expression
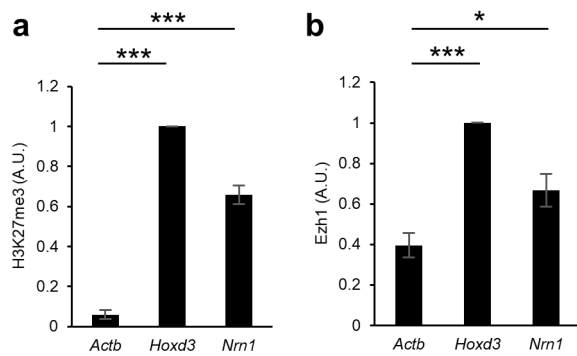
Figure 4. H3K27me3 deposition and Ezh1 binding at *Nrn1* locus in cortical neurons. Cortical neurons isolated from E14.5 mouse cortex and cultured for 10 DIV under differentiation-inducing conditions were subjected to ChIP-qPCR analysis with antibodies to H3K27me3 and Ezh1. ChIP-qPCR analysis of H3K27me3 deposition **(a)** and Ezh1 binding **(b)** at the indicated promoters. *Hoxd3* was examined as a positive control, and *Actb* as a negative control. Data are expressed as arbitrary units normalized against percent input of *Hoxd3* of each experiment. Data are means ± SEM from four independent experiments. Differences were evaluated by one-way ANOVA followed by Dunnett's multiple-comparison test. *p < 0.05, ***p < 0.001.

of *Nrn1* in cortical neurons. Although *Ezh1* regulates the expression of PSD95 and binds to the *Psd95* promoter in the rat hippocampus (*18*), no other reports on target of Ezh1 have been reported in the nervous system. Ezh1 is enriched in the adult mouse brain, and knockdown of Ezh1 in the mouse prefrontal cortex attenuates sociability and promotes motivational behaviors (*28*). However, the molecular mechanisms responsible for these behavior phenotypes are not fully understood. Although *Nrn1* is a direct target of several PRC1 components in Hs68 cells (*40*), *Nrn1* has not been reported to be a direct target of PcG components in post-mitotic cells such as neurons. Our results demonstrate that *Nrn1* is a direct target of PcG components in post-mitotic neurons. It will be of interest to determine whether Ezh1 mediates neuronal maturation of cortical neurons, and if so, whether it does so by regulating Nrn1 expression.

Although Ezh1 and Ezh2 are primarily associated with gene repression, several lines of evidence suggest that they both play non-canonical roles in gene activation (*15,18,20,21*). In myotubes, Ezh1 shows genome-wide association with H3K4me3 and RNA polymerase, and with reduced levels of H3K27me3 (*20*). In rat hippocampal neurons, during neuronal maturation, binding of Ezh1 at the *Psd95* promoter increases concomitantly with acetylation of histone H3 at lysine-27 (H3K27ac) and phosphorylation of histone H3 at serine-28 (H3S28ph), both of which are active histone modifications, although their relationships with Ezh1 are unknown (*18*). Our results show that Ezh1 and H3K27me3 are associated with the *Nrn1* promoter (Figure 4), even though *Nrn1* is expressed in neurons. It is possible that the balance between H3K27me3 and other active histone modification determines the extent of *Nrn1* expression. In future studies, we will seek to

determine whether another histone modification such as H3K4me3, H3K27ac, or H3S28ph is deposited on the *Nrn1* promoter, and if so, whether the amounts of such modifications change during neuronal maturation.

Our RNA-seq data indicate that 3,059 genes were upregulated by Ezh1 cKO, but 86.4% of those were < 3 RPKM on average in cKO samples, suggesting expression of these genes is not high even in derepressed status (Figure 3). Additionally, the level of H3K27me3 did not significantly differ between Ezh1 cKO and control (Figures 2c and 2d). Two studies suggested that Ezh1 depletion alone does not affect the global level of H3K27me3 (*13,22*), suggesting a compensatory role of Ezh2 upon *Ezh1* deletion. In MSNs, *Ezh1* and *Ezh2* double deletion leads to a dramatic decrease in the level of H3K27me3 and upregulation of death-promoting genes and associated neurodegenerative changes (*22*). *Ezh1* and *Ezh2* double deletion may also lead to a global decrease in the level of H3K27me3 in cortical neurons and more robust derepression of their common target genes. Moreover, other genes related to neuronal maturation were downregulated by Ezh1 cKO (Figure 3), although Ezh1 did not bind directly to their promoters (data not shown). It is possible that these genes were affected by downregulation of Nrn1. In future work, we will investigate whether these genes contribute to the defects in neuronal maturation caused by Ezh1 cKO.

Nrn1 has been reported to be down-regulated by chronic stress which worsen depression, and in the cerebral cortex and hippocampus of patients with Alzheimer's disease (*46,47*). Moreover, viral-mediated expression of Nrn1 in the hippocampus reduced symptoms of these diseases (*46,47*). Therefore, given that Ezh1 regulates Nrn1 expression, up-regulation of Ezh1 expression may treat these disorders.

In conclusion, we showed that expression of Ezh1 increases during neuronal maturation and that Ezh1 positively regulates transcription of *Nrn1*. Future studies will elucidate the role of Ezh1-mediated regulation of Nrn1 in the context of neuronal maturation.

References

1. Florio M, Huttner WB. Neural progenitors, neurogenesis and the evolution of the neocortex. Development. 2014; 141:2182-2194.

2. Feldmeyer D, Radnikow G. Developmental alterations in the functional properties of excitatory neocortical synapses. J Physiol. 2009; 587:1889-1896.

3. Parekh R, Ascoli GA. Quantitative investigations of axonal and dendritic arbors: development, structure, function, and pathology. Neuroscientist. 2015; 21:241-254.

4. Sekine K, Kubo K, Nakajima K. How does Reelin control neuronal migration and layer formation in the developing mammalian neocortex? Neurosci Res. 2014; 86:50-58.

5. Kaur P, Karolina DS, Sepramaniam S, Armugam A, Jeyaseelan K. Expression profiling of RNA transcripts during neuronal maturation and ischemic injury. PLoS One. 2014; 9:e103525.

6. Hsieh J, Gage FH. Chromatin remodeling in neural development and plasticity. Curr Opin Cell Biol. 2005; 17:664-671.

7. Kishi Y, Gotoh Y. Regulation of chromatin structure during neural development. Front Neurosci. 2018; 12:874.

8. Tyssowski K, Kishi Y, Gotoh Y. Chromatin regulators of neural development. Neuroscience. 2014; 264:4-16.

9. Di Croce L, Helin K. Transcriptional regulation by Polycomb group proteins. Nat Struct Mol Biol. 2013; 20:1147-1155.

10. Simon JA, Kingston RE. Occupying chromatin: Polycomb mechanisms for getting to genomic targets, stopping transcriptional traffic, and staying put. Mol Cell. 2013; 49:808-824.

11. Bernstein BE, Mikkelsen TS, Xie X, *et al.* A bivalent chromatin structure marks key developmental genes in embryonic stem cells. Cell. 2006; 125:315-326.

12. Zaidi SK, Frietze SE, Gordon JA, Heath JL, Messier T, Hong D, Boyd JR, Kang M, Imbalzano AN, Lian JB, Stein JL, Stein GS. Bivalent epigenetic control of oncofetal gene expression in cancer. Mol Cell Biol. 2017; 37:e00352-17.

13. Margueron R, Li G, Sarma K, Blais A, Zavadil J, Woodcock CL, Dynlacht BD, Reinberg D. Ezh1 and Ezh2 maintain repressive chromatin through different mechanisms. Mol Cell. 2008; 32:503-518.

14. Shen X, Liu Y, Hsu YJ, Fujiwara Y, Kim J, Mao X, Yuan GC, Orkin SH. EZH1 mediates methylation on histone H3 lysine 27 and complements EZH2 in maintaining stem cell identity and executing pluripotency. Mol Cell. 2008; 32:491-502.

15. Xu J, Shao Z, Li D, Xie H, Kim W, Huang J, Taylor JE, Pinello L, Glass K, Jaffe JD, Yuan GC, Orkin SH. Developmental control of polycomb subunit composition by GATA factors mediates a switch to non-canonical functions. Mol Cell. 2015; 57:304-316.

16. Attwooll C, Oddi S, Cartwright P, Prosperini E, Agger K, Steensgaard P, Wagener C, Sardet C, Moroni MC, Helin K. A novel repressive E2F6 complex containing the polycomb group protein, EPC1, that interacts with EZH2 in a proliferation-specific manner. J Biol Chem. 2005; 280:1199-1208.

17. Bracken AP, Pasini D, Capra M, Prosperini E, Colli E, Helin K. EZH2 is downstream of the pRB-E2F pathway, essential for proliferation and amplified in cancer. EMBO J. 2003; 22:5323-5335.

18. Henriquez B, Bustos FJ, Aguilar R, Becerra A, Simon F, Montecino M, van Zundert B. Ezh1 and Ezh2 differentially regulate PSD-95 gene transcription in developing hippocampal neurons. Mol Cell Neurosci. 2013; 57:130-143.

19. Hidalgo I, Herrera-Merchan A, Ligos JM, Carramolino L, Nunez J, Martinez F, Dominguez O, Torres M, Gonzalez S. Ezh1 is required for hematopoietic stem cell maintenance and prevents senescence-like cell cycle arrest. Cell Stem Cell. 2012; 11:649-662.

20. Mousavi K, Zare H, Wang AH, Sartorelli V. Polycomb protein Ezh1 promotes RNA polymerase II elongation. Mol Cell. 2012; 45:255-262.

21. Stojic L, Jasencakova Z, Prezioso C, Stutzer A, Bodega B, Pasini D, Klingberg R, Mozzetta C, Margueron R, Puri PL, Schwarzer D, Helin K, Fischle W, Orlando V. Chromatin regulated interchange between polycomb repressive complex 2 (PRC2)-Ezh2 and PRC2-Ezh1 complexes controls myogenin activation in skeletal muscle cells. Epigenetics Chromatin. 2011; 4:16.

22. von Schimmelmann M, Feinberg PA, Sullivan JM, Ku SM, Badimon A, Duff MK, Wang Z, Lachmann A, Dewell S, Ma'ayan A, Han MH, Tarakhovsky A, Schaefer A. Polycomb repressive complex 2 (PRC2) silences genes responsible for neurodegeneration. Nat Neurosci. 2016; 19:1321-1330.

23. Hirabayashi Y, Suzki N, Tsuboi M, Endo TA, Toyoda T, Shinga J, Koseki H, Vidal M, Gotoh Y. Polycomb limits the neurogenic competence of neural precursor cells to promote astrogenic fate transition. Neuron. 2009; 63:600-613.

24. Morimoto-Suzki N, Hirabayashi Y, Tyssowski K, Shinga J, Vidal M, Koseki H, Gotoh Y. The polycomb component Ring1B regulates the timed termination of subcerebral projection neuron production during mouse neocortical development. Development. 2014; 141:4343-4353.

25. Pereira JD, Sansom SN, Smith J, Dobenecker MW, Tarakhovsky A, Livesey FJ. Ezh2, the histone methyltransferase of PRC2, regulates the balance between self-renewal and differentiation in the cerebral cortex. Proc Natl Acad Sci U S A. 2010; 107:15957-15962.

26. Wang Z, Zhang Y, Fang J, Yu F, Heng D, Fan Y, Xu J, Peng B, Liu W, Han S, He X. Decreased methylation level of H3K27me3 increases seizure susceptibility. Mol Neurobiol. 2017; 54:7343-7352.

27. Di Meglio T, Kratochwil CF, Vilain N, Loche A, Vitobello A, Yonehara K, Hrycaj SM, Roska B, Peters AH, Eichmann A, Wellik D, Ducret S, Rijli FM. Ezh2 orchestrates topographic migration and connectivity of mouse precerebellar neurons. Science. 2013; 339:204-207.

28. Johnstone AL, O'Reilly JJ, Patel AJ, Guo Z, Andrade NS, Magistri M, Nathanson L, Esanov R, Miller BH, Turecki G, Brothers SP, Zeier Z, Wahlestedt C. EZH1 is an antipsychotic-sensitive epigenetic modulator of social and motivational behavior that is dysregulated in schizophrenia. Neurobiol Dis. 2018; 119:149-158.

29. Goebbels S, Bormuth I, Bode U, Hermanson O, Schwab MH, Nave KA. Genetic targeting of principal neurons in neocortex and hippocampus of NEX-Cre mice. Genesis. 2006; 44:611-621.

30. Mishina M, Sakimura K. Conditional gene targeting on the pure C57BL/6 genetic background. Neurosci Res. 2007; 58:105-112.

31. Eto H, Kishi Y, Yakushiji-Kaminatsui N, Sugishita H,

Utsunomiya S, Koseki H, Gotoh Y. The Polycomb group protein Ring1 regulates dorsoventral patterning of the mouse telencephalon. Nat Commun. 2020; 11:5709.

32. Kim D, Paggi JM, Park C, Bennett C, Salzberg SL. Graph-based genome alignment and genotyping with HISAT2 and HISAT-genotype. Nat Biotechnol. 2019; 37:907-915.

33. Liao Y, Smyth GK, Shi W. featureCounts: an efficient general purpose program for assigning sequence reads to genomic features. Bioinformatics. 2014; 30:923-930.

34. Robinson MD, McCarthy DJ, Smyth GK. edgeR: a Bioconductor package for differential expression analysis of digital gene expression data. Bioinformatics. 2010; 26:139-140.

35. McCarthy DJ, Chen Y, Smyth GK. Differential expression analysis of multifactor RNA-Seq experiments with respect to biological variation. Nucleic Acids Res. 2012; 40:4288-4297.

36. Huang da W, Sherman BT, Lempicki RA. Systematic and integrative analysis of large gene lists using DAVID bioinformatics resources. Nat Protoc. 2009; 4:44-57.

37. Huang da W, Sherman BT, Lempicki RA. Bioinformatics enrichment tools: paths toward the comprehensive functional analysis of large gene lists. Nucleic Acids Res. 2009; 37:1-13.

38. Wu SX, Goebbels S, Nakamura K, Nakamura K, Kometani K, Minato N, Kaneko T, Nave KA, Tamamaki N. Pyramidal neurons of upper cortical layers generated by NEX-positive progenitor cells in the subventricular zone. Proc Natl Acad Sci U S A. 2005; 102:17172-17177.

39. Sakai H, Fujii Y, Kuwayama N, Kawaji K, Gotoh Y, Kishi Y. Plag1 regulates neuronal gene expression and neuronal differentiation of neocortical neural progenitor cells. Genes Cells. 2019; 24:650-666.

40. Pemberton H, Anderton E, Patel H, Brookes S, Chandler H, Palermo R, Stock J, Rodriguez-Niedenfuhr M, Racek T, de Breed L, Stewart A, Matthews N, Peters G. Genome-wide co-localization of Polycomb orthologs and their effects on gene expression in human fibroblasts. Genome Biol. 2014; 15:R23.

41. Harwell C, Burbach B, Svoboda K, Nedivi E. Regulation of cpg15 expression during single whisker experience in the barrel cortex of adult mice. J Neurobiol. 2005; 65:85-96.

42. Nedivi E, Fieldust S, Theill LE, Hevron D. A set of genes expressed in response to light in the adult cerebral cortex and regulated during development. Proc Natl Acad Sci U S A. 1996; 93:2048-2053.

43. Subramanian J, Michel K, Benoit M, Nedivi E. CPG15/Neuritin mimics experience in selecting excitatory synapses for stabilization by facilitating PSD95 recruitment. Cell Rep. 2019; 28:1584-1595.e5.

44. Fujino T, Leslie JH, Eavri R, Chen JL, Lin WC, Flanders GH, Borok E, Horvath TL, Nedivi E. CPG15 regulates synapse stability in the developing and adult brain. Genes Dev. 2011; 25:2674-2685.

45. Picard N, Leslie JH, Trowbridge SK, Subramanian J, Nedivi E, Fagiolini M. Aberrant development and plasticity of excitatory visual cortical networks in the absence of cpg15. J Neurosci. 2014; 34:3517-3522.

46. Choi Y, Lee K, Ryu J, Kim HG, Jeong AY, Woo RS, Lee JH, Hyun JW, Hahn S, Kim JH, Kim HS. Neuritin attenuates cognitive function impairments in tg2576 mouse model of Alzheimer's disease. PLoS One. 2014; 9:e104121.

47. Son H, Banasr M, Choi M, *et al*. Neuritin produces antidepressant actions and blocks the neuronal and behavioral deficits caused by chronic stress. Proc Natl Acad Sci U S A. 2012; 109:11378-11383.

48. Hrvatin S, Hochbaum DR, Nagy MA, Cicconet M, Robertson K, Cheadle L, Zilionis R, Ratner A, Borges-Monroy R, Klein AM, Sabatini BL, Greenberg ME. Single-cell analysis of experience-dependent transcriptomic states in the mouse visual cortex. Nat Neurosci. 2018; 21:120-129.

§These authors contributed equally to this work.
Address correspondence to:
Hiroshi Takemoto, Business-Academia Collaborative Laboratory (Shionogi), Graduate School of Pharmaceutical Sciences, The University of Tokyo, 7-3-1 Hongo, Bunkyo-ku, Tokyo, 113-0033, Japan.
E-mail: hiroshi.takemoto@mol.f.u-tokyo.ac.jp